

**OAK RIDGE  
NATIONAL LABORATORY**

MANAGED BY UT-BATTELLE  
FOR THE DEPARTMENT OF ENERGY

**ORNL/TM-2003/128**

## **A Study of the Effects of a Radiation Dispersal Device**

**C. O. Slater  
J. C. Gehin  
R. T. Santoro**



ORNL-27 (4-00)

### DOCUMENT AVAILABILITY

Reports produced after January 1, 1996, are generally available free via the U.S. Department of Energy (DOE) Information Bridge:

**Web site:** <http://www.osti.gov/bridge>

Reports produced before January 1, 1996, may be purchased by members of the public from the following source:

National Technical Information Service  
5285 Port Royal Road  
Springfield, VA 22161  
**Telephone:** 703-605-6000 (1-800-553-6847)  
**TDD:** 703-487-4639  
**Fax:** 703-605-6900  
**E-mail:** [info@ntis.fedworld.gov](mailto:info@ntis.fedworld.gov)  
**Web site:** <http://www.ntis.gov/support/ordernowabout.htm>

Reports are available to DOE employees, DOE contractors, Energy Technology Data Exchange (ETDE) representatives, and International Nuclear Information System (INIS) representatives from the following source:

Office of Scientific and Technical Information  
P.O. Box 62  
Oak Ridge, TN 37831  
**Telephone:** 865-576-8401  
**Fax:** 865-576-5728  
**E-mail:** [reports@adonis.osti.gov](mailto:reports@adonis.osti.gov)  
**Web site:** <http://www.osti.gov/contact.html>

This report was prepared as an account of work sponsored by an agency of the United States Government. Neither the United States government nor any agency thereof, nor any of their employees, makes any warranty, express or implied, or assumes any legal liability or responsibility for the accuracy, completeness, or usefulness of any information, apparatus, product, or process disclosed, or represents that its use would not infringe privately owned rights. Reference herein to any specific commercial product, process, or service by trade name, trademark, manufacturer, or otherwise, does not necessarily constitute or imply its endorsement, recommendation, or favoring by the United States Government or any agency thereof. The views and opinions of authors expressed herein do not necessarily state or reflect those of the United States Government or any agency thereof.

Nuclear Science and Technology Division (94)

**A STUDY OF THE EFFECTS OF A  
RADIATION DISPERSAL DEVICE**

C. O. Slater  
J. C Gehin  
R. T. Santoro

Oak Ridge National Laboratory  
Oak Ridge, Tennessee 37831

Date Published: May 2003

Prepared by the  
OAK RIDGE NATIONAL LABORATORY  
P.O. Box 2008  
Oak Ridge, Tennessee 37831-6285  
managed by  
UT-Battelle, LLC  
for the  
U.S. DEPARTMENT OF ENERGY  
under contract DE-AC05-00OR22725

Page Intentionally Blank

## TABLE OF CONTENTS

LIST OF TABLES .....	v
LIST OF FIGURES .....	vii
ABSTRACT .....	ix
1.0 INTRODUCTION .....	3
2.0 MASH SOURCE FILE FOR RADIOLOGICAL INCIDENT .....	5
2.1 Description of the Radiological Incident .....	5
2.2 MASH Source Definition.....	5
3.0 RADIATION EFFECTS FROM DEPOSITED SOURCES.....	9
3.1 Free-Field Fluence Calculation.....	9
3.2 Adjoint Calculations .....	9
3.3 Coupling Calculations.....	10
3.4 Results.....	10
3.5 Alternative Coupling Method and Results.....	11
4.0 CONCLUSIONS.....	29
5.0 REFERENCES.....	31

Page Intentionally Blank

## LIST OF TABLES

<b>Table</b>	<b>Page</b>
2.1 HPAC particle size distribution for <sup>137</sup> Cs salt/powder.....	6
2.2 Photon source from <sup>137</sup> Cs with equilibrium decay nuclides.....	7
2.3 Energy group boundaries for the ORIGEN2 group structure .....	8
3.1 ANSI standard dose rate and protection factors for commander’s head position as a function of vehicle location and orientation (no contributions from fallout on vehicle).....	13
3.2 ANSI standard dose rate and protection factors for commander’s head position as a function of vehicle location and orientation (includes contributions from fallout on vehicle) .....	14
3.3 ANSI standard dose rate and protection factors for commander’s head position as a function of vehicle location and orientation (includes contributions from fallout on vehicle and on ground inside MASH-MORSE geometry model).....	15
3.4 ANSI standard dose rate and protection factors for driver’s head position as a function of vehicle location and orientation (no contributions from fallout on vehicle).....	16
3.5 ANSI standard dose rate and protection factors for driver’s head position as a function of vehicle location and orientation (includes contributions from fallout on vehicle) .....	17
3.6 ANSI standard dose rate and protection factors for driver’s head position as a function of vehicle location and orientation (includes contributions from fallout on vehicle and on ground inside MASH-MORSE geometry model).....	18

Page Intentionally Blank

## LIST OF FIGURES

Figure		Page
2.1	HPAC distribution of the ground source for Cs-137 radiological weapon event.....	6
2.2	Energy spectrum ( $s^{-1}$ ) for a 10-kCi $^{137}\text{Cs}$ source .....	8
3.1	Photon isodose-rate contours for a horizontal plane 3m above the ground due to the detonation and dispersal of a 10-kCi $^{137}\text{Cs}$ source.....	19
3.2	Photon isodose-rate contours for a horizontal plane 325m above the ground due to the detonation and dispersal of a 10-kCi $^{137}\text{Cs}$ source.....	20
3.3	Photon isodose-rate contours for a vertical plane 325m left of the origin due to the detonation and dispersal of a 10-kCi $^{137}\text{Cs}$ source.....	21
3.4	Photon isodose-rate contours for a vertical plane 375m right of the origin due to the detonation and dispersal of a 10-kCi $^{137}\text{Cs}$ source.....	22
3.5	Model of the composite material armored assault vehicle used in the analysis .....	23
3.6	Cutaway view of the model of the composite material armored assault vehicle used in the analysis. The model shows the crew and infantry locations.....	24
3.7	Approximate locations of the armored vehicle within the radiation field for the results shown in Tables 3.1-3.7 .....	25
3.8	Free-field and shielded fluence spectra at the commander's head position for a vehicle located near the detonation site for the 10-kCi $^{137}\text{Cs}$ weapon (x=10 m and y=10 m, $0^\circ$ orientation angle) .....	26
3.9	Free-field and shielded fluence spectra at the commander's head position for a vehicle located at a large distance from the detonation site for the 10-kCi $^{137}\text{Cs}$ weapon (x=-400 m and y=400 m, $0^\circ$ orientation angle).....	27

Page Intentionally Blank

# **A STUDY OF THE EFFECTS OF A RADIATION DISPERSAL DEVICE**

C. O. Slater  
J. C. Gehin  
R. T. Santoro

## **ABSTRACT**

The effects of radiation from the detonation of a radiation dispersal device were examined through the coupling of computer code systems. The HPAC code system modeled the dispersal of radioactive particles from the detonation and output the data over a grid. The ORIGEN2 code calculated the photon spectrum per unit of material which when coupled with the HPAC data yielded the photon source spectra per unit area per second. The source spectra were reformulated as a volumetric source for the TORT code, which was used to calculate free-field fluences over a large region. The DRC3B code coupled those fluences with MASH-MORSE adjoint leakages from an armored vehicle to determine fluences, dose rates, and protection factors at selected positions within the vehicle as a function of location and orientation with respect to the detonation point. Indications are that meaningful results can be obtained within a reasonable amount of time using an advanced computer system.

Page Intentionally Blank

## 1.0 INTRODUCTION

Concern has been voiced about terrorists detonating so-called dirty bombs [or radiation dispersal devices (RDDs)] and about the effects the dispersed radiation might have on people in the area. Therefore, a study was begun recently to examine the effects of one such type of device. First, a dispersal pattern for the postulated device was developed and the corresponding radiation source was determined. Then, free-field fluences due to the source were calculated over a large volume, and the dose rates and protection factors within an armored vehicle located at various points within the radiation field were determined. The following sections describe the source, the transport calculation, the adjoint calculations, the coupling calculations, and the resulting calculated free-field and shielded dose rates at selected locations.

The analysis of radiation dispersal devices has now become part of the NATO Allied Engineering-14 document,<sup>1</sup> which gives the military vehicle designer guidelines for improving radiation protection.

Page Intentionally Blank

## 2.0 MASH SOURCE FILE FOR RADIOLOGICAL INCIDENT

The first task involved the determination of the radiation source that would result from the detonation of an RDD during assumed atmospheric conditions. The Hazard Prediction Assessment Capability (HPAC) code system<sup>2</sup> has the capability to provide modeling of the dispersal of radioactive materials that may result from a terrorist event. In order to demonstrate the creation of a radioactive ground source with HPAC for use by the MASH code system,<sup>3</sup> we modeled a terrorist event with HPAC and the resulting ground deposition was exported to create a source term for the MASH code system.

### 2.1 Description of the Radiological Incident

The assumed incident for the generation of the source involves the release of <sup>137</sup>Cs with high explosives and then the atmospheric dispersion of that <sup>137</sup>Cs by the prevailing winds. The source was assumed to consist of 10,000 Ci of <sup>137</sup>Cs in the form of a powder that is initially dispersed with 22.7 kg (50 lb) of high explosives. The winds are out of the south-southeast and the resulting plume spreads materials over a region of about one square kilometer. The source characterization parameters have been arbitrarily selected, but may represent a credible terrorist event. The surface deposition calculated by HPAC is shown in Figure 2.1. Note that the detonation occurs at the origin of the system with the x-axis across the page and y-axis up the page.

### 2.2 MASH Source Definition

The incident described in Section 2.1 was modeled using the HPAC radiological weapon (RWP) source term model. This model created the initial dispersion of the <sup>137</sup>Cs material by the explosion for input to the atmospheric dispersion model, SCIPUFF. SCIPUFF (Second-order Closure Integrated PUFF) is a Lagrangian transport and diffusion model for atmospheric dispersion applications. The numerical technique used to solve the dispersion model equations is the Gaussian puff method in which a collection of three-dimensional puffs is used to represent an arbitrary time-dependent concentration field. SCIPUFF also uses a turbulent diffusion parameterization based on second-order turbulence closure theories, which provides a probabilistic capability allowing the prediction of the concentration fluctuation variance. The RWP model uses the particle size distribution given in Table 2.1 for <sup>137</sup>Cs salt/powder.

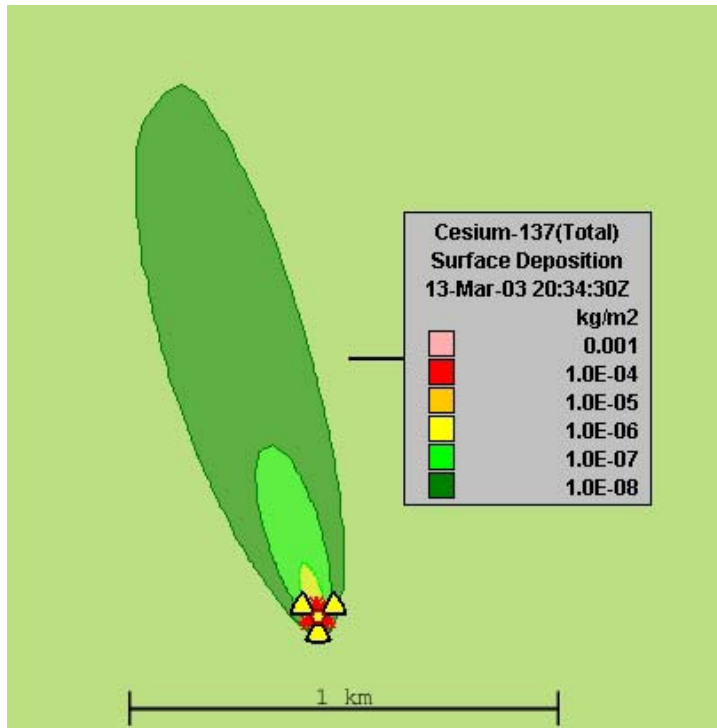


**Figure 2.1. HPAC distribution of the ground source for Cs-137 radiological weapon event.**

The source material for this incident,  $^{137}\text{Cs}$  (half-life 30 years), has a specific activity of about 87 Ci/g. However, the decay of  $^{137}\text{Cs}$  also creates  $^{137\text{m}}\text{Ba}$ , which has a relatively short half-life (2.5 minutes) and therefore quickly reaches equilibrium concentration with  $^{137}\text{Cs}$ . Therefore, the specific activity of the source term is 169 Ci/g when taking the equilibrium nuclides into account. The ORIGEN2 code<sup>4</sup> was used to compute the photon release from one kilogram of  $^{137}\text{Cs}$  (including equilibrium nuclides) in an 18-energy-group structure. The computed photon source is shown in Table 2.2 and the spectrum is plotted in Figure 2.2. This photon source information was combined with ground-deposition information from HPAC to create a ground photon source to be used by the MASH code system. The energy boundaries for the group structure are given in Table 2.3. These data are needed for the conversion of the source to a group structure for which a cross-section library is available.

**Table 2.1. HPAC particle size distribution for  $^{137}\text{Cs}$  salt/powder.**

Particle size range (microns)	Fraction of mass in range
0 - 1	1.11E-11
1 - 5	3.11E-05
5 - 10	0.002177
10 - 20	0.043375
20 - 30	0.110141
30 - 60	0.402039
60 - 100	0.283177
100 - 175	0.132431
175 - 400	0.026167
Total	0.999539

**Table 2.2. photon source from  $^{137}\text{Cs}$  with equilibrium decay nuclides.**

Energy Group	Avg Energy (MeV)	Photons ( $\text{s}^{-1} \text{kg}^{-1}$ )	Energy Group	Avg Energy (MeV)	Photons ( $\text{s}^{-1} \text{kg}^{-1}$ )
1	9.5	0.0	10	0.575	3.136+15
2	7.0	0.0	11	0.375	1.452+12
3	5.0	0.0	12	0.225	9.688+12
4	3.5	0.0	13	0.125	1.220+13
5	2.75	0.0	14	0.085	2.327+13
6	2.25	0.0	15	0.0575	4.667+13
7	1.75	0.0	16	0.0375	2.349+14
8	1.25	6.856+7 <sup>a</sup>	17	0.0250	6.019+13
9	0.85	1.799+10	18	0.0100	3.328+14

<sup>a</sup>Read as  $6.856 \times 10^7$ .

**Table 2.3. Energy group boundaries for the ORIGEN2 group structure.**

Energy Group	Upper Energy (MeV)	Energy Group	Upper Energy (MeV)
1	11.0	10	0.7
2	8.0	11	0.45
3	6.0	12	0.3
4	4.0	13	0.15
5	3.0	14	0.1
6	3.5	15	0.07
7	2.0	16	0.045
8	1.5	17	0.03
9	1.0	18	0.02 <sup>a</sup>

<sup>a</sup>Even though the average energy is given as 0.01 MeV (meaning the lower boundary is 0.0 MeV), the lower energy was selected as 0.01 MeV, which is the lower limit for most photon cross-section libraries.

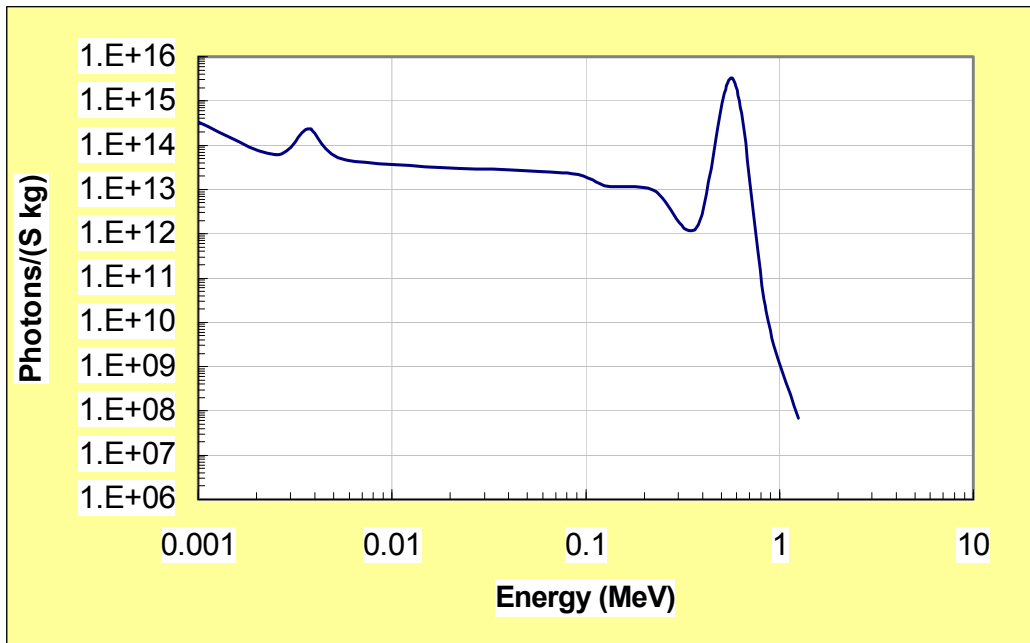


**Figure 2.2. Energy spectrum ( $s^{-1}$ ) for a 10-kCi <sup>137</sup>Cs source.**

### 3.0 RADIATION EFFECTS FROM DEPOSITED SOURCES

The radiation effects from the deposited sources were determined using a previously developed procedure that was modified for the current study. This procedure involved the coupling of free-field directional fluences with adjoint leakages from a vehicle or structure. Details of the calculations follow.

#### 3.1 Free-Field Fluence Calculation

To perform the free-field fluence calculation, one needs a source in the proper format. Therefore, the HPAC source data were stored in a file with the GENMASH<sup>5</sup> format. Then, the modified GENTORT code<sup>6</sup> (modified to accept either a file having only a ground source or one having both ground and airborne sources) was used to create a source for the TORT<sup>7</sup> three-dimensional radiation transport code, which would calculate the free-field fluences. The GENTORT code was also modified to place half of the source in mesh cells in each of two k-levels, one above and one below the ground plane. This was a substitute for an internal k-boundary flux file to represent a plane source at ground level (a feature that has not been implemented in TORT for practical usage). It is left to the user to select adequately spaced k-mesh about the ground level and to create a separate zone for the top k-interval within the ground so that the ground density can be adjusted appropriately.

The TORT calculation was performed using the last 11 groups of the DABL69<sup>8</sup> 23-group photon structure, the weighted-difference method, a symmetric  $S_{12}$  quadrature set (192 directions), and a  $P_5$  Legendre polynomial expansion of the scattering cross sections. Only air and ground mixtures were required for this calculation. A point flux convergence criterion of 0.001 and an inner iteration limit of 12 were selected, and the convergence criterion was satisfied by the bottom six groups of the 11-group structure. The key fluxes were converged (to three decimal places) for all groups. The computational model consisted of a  $78 \times 80 \times 40$  x-y-z spatial mesh (spanning a region defined by  $-1.5 \text{ km} \leq x \leq 1.5 \text{ km}$ ,  $-0.85 \text{ km} \leq y \leq 2.25 \text{ km}$ , and  $-0.0005 \text{ km} \leq z \leq 1.0 \text{ km}$ ). The calculation for this mesh required about 65.5 minutes on our fastest IBM workstation (an IBM p630 dual processor workstation with dual 1.0 GHz Power-4 CPUs and 2 GB Memory). Directional fluences were output for a  $38 \times 38 \times 15$  submesh of the original geometry. The TORT x- and y- axes are aligned with those of the HPAC source geometry shown in Figure 2.1. The TORT origin is at the center of detonation.

Contour plots of the free-field dose rates calculated from the TORT fluences are shown in Figures 3.1 and 3.2 for horizontal planes and in Figures 3.3 and 3.4 for vertical planes. The horizontal views show that the dose-rate profile closely follows the source distribution calculated by HPAC (Figure 2.1). All the views show that there is relatively little problem with ray effects. There are finer symmetric quadrature sets available that could be used decrease the minor ray effects seen in the figures. However, since the effects are minor and this is a preliminary study, it was judged that additional calculations using the refined quadratures were not required.

#### 3.2 Adjoint Calculations

The MASH-MORSE adjoint calculations were performed for fluences and dose rates at the head positions of a commander and driver within the armored vehicle pictured in Figures 3.5 and 3.6. The same 11-group structure and microscopic cross-section library used by the TORT calculation were used by the MASH-MORSE adjoint calculations. The materials required by MASH-MORSE were mixed (in adjoint mode) using the XCHEKER code, which is a modified

version of the XCHEKR code<sup>9</sup> that served as an auxiliary mixing code for the original MORSE. For each case, five million histories were followed, leading to about 2.3-million escapes for each calculation. In addition to data for particles escaping the system being written to the history file, data for particles crossing the ground surface were also written. The latter data were to be used to assess what contribution fallout on the ground within the MASH-MORSE geometry makes to the dose rate at the location of interest. The contribution should be relatively small if the ground surface within the model does not extend very far beyond the vehicle or structure and there are no steep gradients in the source distribution over the ground surface.

One of these calculations required about 506 minutes on an older IBM workstation while the other required about 105 minutes on our fastest workstation. Both required significantly more time than did the TORT calculation.

### 3.3 Coupling Calculations

The DRC3B code, an update of the DRC3 code,<sup>3</sup> was used to perform the coupling of the TORT free-field fluences (Sect. 3.1) and the MASH-MORSE adjoint leakages (Sect. 3.2). The update allows the contributions of fallout on a surface to be included along with the contributions from direct and scattered contributions. The user is allowed to specify the z-locations of the fallout surfaces and the normal component for each surface (A +1 means upward crossings add and downward crossing subtract while -1 means downward crossings add and upward crossings subtract. The interior ground surface is the only surface from which one would expect both positive and negative contributions).

One or more preliminary calculations are required prior to the coupling. First, one runs VIST3D<sup>3</sup> to produce 3-D directional fluence arrays over a spatial volume that would encompass all parts of the MASH-MORSE geometry for all of the selected positions and orientations. DRC3B interpolates those data to calculate the directional fluence values needed to couple with the MASH-MORSE adjoint leakages. Second, if fallout contributions are to be included, one needs to run the PLATEQ code<sup>6</sup> to generate a fallout source distribution over the same spatial mesh used in the VIST3D calculation. DRC3B interpolates these data to get the appropriate source at the MASH-MORSE leakage location. The source is converted to directional fluence by dividing it by the cosine that the adjoint leakage particle makes with the surface.

At the user's option, DRC3B calculates free-field and shielded fluence and dose-rate spectra, free-field and shielded integrated fluence and dose rate, and fluence and dose-rate protection factors. The option that produces spectra yields a large volume of printed output per detector position.

The coupling calculations produced results for 76 range/orientations (four orientations for each of 19 locations), requiring 27 to 36 minutes of computation time on our fastest IBM workstation. More time was required when fallout was considered than was required when it was not. The processing of the large number of events on the MASH-MORSE history file contributes greatly to the time required for the coupling calculations.

### 3.4 Results

For the commander's head position, results are presented in Tables 3.1, 3.2, and 3.3 for four orientations of the vehicle at each of seven vehicle locations. The approximate locations of the vehicle are shown in Figure 3.7. Note that the shape representing the vehicle is not to scale (the shape is about 60 m wide and 120 m long according to the scale given on the figure). The

results in Table 3.1 are for the case that included no fallout on a surface above the vehicle. The results in Table 3.2 are for the case that included fallout on a surface above the vehicle. The results in Table 3.3 are for the case that included fallout on a surface above the vehicle as well as on the ground within the MASH-MORSE geometry model. Results for the Driver's head position are shown in Tables 3.4, 3.5, and 3.6. For the commander's head position, the free-field dose rates vary only 4 to 6% with orientation except for the 15% variation at the second vehicle location and the 76% variation at the third vehicle location. In general, shielded dose rates vary 10 to 30% at all except the third vehicle location where the variation is 90 to 106%. At several locations, fallout on the vehicle adds relatively large contributions to the dose rate inside the vehicle. The contribution from fallout on the ground is also significant for several vehicle locations. With the exception of the 189% variation for the third vehicle location for the case without fallout atop the vehicle, variations in the protection factors range between 6 and 25%. The large protection factor for the 0-degree orientation at location 3 is believed to be due to the shielding provided the commander by the metal in the engine. Variations in the free-field dose rate for the driver's head position are smaller than those for the commander's head position (7% at the second vehicle location, 39% at the third vehicle location, and 2 to 4% at the other vehicle locations). However, variations in the shielded dose rates and the protection factors are generally larger (14 to 65% versus 6 to 30% at all vehicle locations except for the third location where results are mixed).

Free-field and shielded fluence spectra at the commander's head position for a vehicle near to and distant from the detonation point are shown in Figures 3.8 and 3.9. The figures show first that fallout on the vehicle adds a lot to the shielded fluence when the vehicle is near the detonation point. A much smaller contribution is made at the distant location. Second, the figures show that photons with energies near the source energy dominate the spectra near the detonation point, but photons with lower energies dominate the spectra at the distant location. Scattered radiation is more important at the distant location than it is at locations near the point of detonation. With the shift in the energy spectra, one would expect the protection factors to be substantially different at the two locations. Such was the case in Table 3.1, but it was less so in Tables 3.2 and 3.3.

### **3.5 Alternative Coupling Method and Results**

For the seven vehicle locations for which results are shown in Tables 3.1-3.6, alternative calculations were performed with the DRC4B code (a modified version of the DRC4 code<sup>6</sup>). The DRC4B code uses a method that is approximate but is generally faster and simpler than the method used in DRC3B. Previous comparisons of the two methods were favorable,<sup>6</sup> so, DRC4B is used here as a check for the more rigorous method used in DRC3B. Directional fluences were calculated at either 27 (3-cubed) or 729 (9-cubed) points surrounding the vehicle at each location. Fallout sources were also restricted to the points that lay on the relevant surfaces. As stated in the report describing DRC4, the results do not include any contributions from ground scatter. In addition, since the source varies significantly over relatively small distances, the integration mesh used by DRC4B might over-represent or under-represent the contributions from the peak source region. The 729-point calculations required about 360 minutes each (on our fastest IBM workstation) for the commander's head calculations without and with fallout on the vehicle. The calculations for the driver's head required only 8 to 9 minutes, since they used the directional fluences from the commander's head calculations. These computational times are much greater than that required by TORT. Timewise, therefore, there is no advantage to using the approximate method.

The DRC4B-calculated dose rates are lower than those calculated by DRC3B. Free-field dose rates calculated by DRC3B are factors of 2.4 to 2.6 higher for the vehicle location near the detonation (location 3) and factors of 21 to 22.5 higher for a vehicle at location 5. Ratios of protection factors calculated by DRC4B to those calculated by DRC3B (with and without fallout on the vehicle) for vehicle locations 1 and 2 range from 0.8 to 1.21 except for the ratio of 1.39 for the driver's head position at vehicle location 2 and the 270° orientation. Elsewhere, ratios for the commander's head position in a vehicle without fallout above it are 1.22-1.34 for location 3, 1.35-1.49 for location 4, 1.66-1.8 for location 5, 1.95-2.16 for location 6, and 1.39-1.45 for location 7. For the driver's head position, those ratios are 1.1-1.28 for location 3, 1.28-1.44 for location 4, 1.48-1.61 for location 5, 1.66-1.78 for location 6, and 1.3-1.33 for location 7. Ratios of protection factors for the commander's head position range from 0.47 to 0.61 for vehicle locations 3-6 and from 1.39 to 1.45 for vehicle location 7. Those for the driver's head position range from 0.49 to 0.72 for vehicle locations 3-6 and from 1.29 to 1.32 for vehicle location 7. For vehicle location 7, fallout contributed little to the dose rate inside the vehicle. Therefore, the protection factor ratios are about the same with or without fallout. Fallout contributions are also small for locations 1 and 2. For the commander's head position, the contributions are less than 1% for location 1 and less than 5.5% for location 2. DRC4B free-field dose rates calculated using the 729-point fluence field differed from those calculated using the 27-point fluence field by 11% or less except at vehicle location 7. There the dose rates increased by 28% at the commander's head position and by 18.5% at the driver's head position. These results indicate that the source integration mesh is more in need of refinement than is the fluence mesh. The favorable comparisons in the previous work were probably due to a source spatial distribution that was more uniform than that for the source used in the present analysis.

**Table 3.1. ANSI standard dose rate and protection factors for commander's head position as a function of vehicle location and orientation (no contributions from fallout on vehicle).**

Vehicle Location (m) <sup>a</sup>		Vehicle Orientation Angle (deg.)	Free-Field Dose Rate (mrem/h)	Shielded Dose Rate (mrem/h)	Protection Factor
x	y				
-100.0	-50.0	0	19.06	3.640	5.236
		90	19.28	4.332	4.451
		180	20.21	4.739	4.264
		270	19.97	4.480	4.457
0.0	-50.0	0	55.35	10.63	5.206
		90	52.83	10.12	5.219
		180	57.34	12.99	4.415
		270	60.92	12.20	4.994
10.0	10.0	0	4756.0	195.0	24.40
		90	3499.0	238.6	14.67
		180	2697.0	319.6	8.439
		270	3631.0	370.3	9.805
-200.0	100.0	0	11.81	2.261	5.224
		90	12.17	2.652	4.590
		180	12.56	2.649	4.741
		270	12.18	2.281	5.340
-400.0	200.0	0	1.289	0.2465	5.231
		90	1.322	0.2905	4.550
		180	1.350	0.2914	4.634
		270	1.317	0.2510	5.247
-400.0	400.0	0	2.728	0.3894	7.006
		90	2.802	0.4379	6.400
		180	2.900	0.4377	6.626
		270	2.824	0.3915	7.212
400.0	400.0	0	0.2027	0.04503	4.501
		90	0.1996	0.04158	4.801
		180	0.1944	0.03582	5.428
		270	0.1974	0.04325	4.565

<sup>a</sup>The vehicle locations are with respect to the TORT origin which is located at the center of the detonation. The TORT x- and y-axes are also aligned with the HPAC source geometry.

**Table 3.2. ANSI standard dose rate and protection factors for commander's head position as a function of vehicle location and orientation (includes contributions from fallout on vehicle).**

Vehicle Location (m) <sup>a</sup>		Vehicle Orientation Angle (deg.)	Free-Field Dose Rate (mrem/h)	Shielded Dose Rate (mrem/h)	Protection Factor
x	y				
-100.0	-50.0	0	19.06	3.654	5.215
		90	19.28	4.346	4.436
		180	20.21	4.757	4.248
		270	19.97	4.498	4.439
0.0	-50.0	0	55.35	11.06	5.003
		90	52.83	10.49	5.038
		180	57.34	13.48	4.253
		270	60.92	12.80	4.759
10.0	10.0	0	4756.0	1334.0	3.564
		90	3499.0	820.4	4.265
		180	2697.0	652.2	4.135
		270	3631.0	954.5	3.804
-200.0	100.0	0	11.81	2.459	4.803
		90	12.17	2.856	4.263
		180	12.56	2.885	4.354
		270	12.18	2.510	4.854
-400.0	200.0	0	1.289	0.2621	4.918
		90	1.322	0.3064	4.314
		180	1.350	0.3087	4.375
		270	1.317	0.2680	4.914
-400.0	400.0	0	2.728	0.6840	3.989
		90	2.802	0.7421	3.776
		180	2.900	0.7614	3.809
		270	2.824	0.7049	4.005
400.0	400.0	0	0.2027	0.04505	4.499
		90	0.1996	0.04160	4.798
		180	0.1944	0.03584	5.425
		270	0.1974	0.04327	4.563

<sup>a</sup>The vehicle locations are with respect to the TORT origin which is located at the center of the detonation. The TORT x- and y-axes are also aligned with the HPAC source geometry.

**Table 3.3. ANSI standard dose rate and protection factors for commander's head position as a function of vehicle location and orientation (includes contributions from fallout on vehicle and on ground inside MASH-MORSE geometry model).**

Vehicle Location (m) <sup>a</sup>		Vehicle Orientation Angle (deg.)	Free-Field Dose Rate (mrem/h)	Shielded Dose Rate (mrem/h)	Protection Factor
x	y				
-100.0	-50.0	0	19.06	3.657	5.211
		90	19.28	4.348	4.434
		180	20.21	4.759	4.246
		270	19.97	4.500	4.437
0.0	-50.0	0	55.35	11.13	4.975
		90	52.83	10.54	5.011
		180	57.34	13.55	4.232
		270	60.92	12.88	4.730
10.0	10.0	0	4756.0	1462.0	3.253
		90	3499.0	905.3	3.865
		180	2697.0	709.8	3.800
		270	3631.0	1033.0	3.514
-200.0	100.0	0	11.81	2.488	4.748
		90	12.17	2.885	4.220
		180	12.56	2.917	4.306
		270	12.18	2.542	4.793
-400.0	200.0	0	1.289	0.2644	4.877
		90	1.322	0.3087	4.282
		180	1.350	0.3111	4.342
		270	1.317	0.2704	4.871
-400.0	400.0	0	2.728	0.7264	3.756
		90	2.802	0.7851	3.569
		180	2.900	0.8062	3.597
		270	2.824	0.7490	3.770
400.0	400.0	0	0.2027	0.04505	4.498
		90	0.1996	0.04160	4.798
		180	0.1944	0.03585	5.425
		270	0.1974	0.04327	4.563

<sup>a</sup>The vehicle locations are with respect to the TORT origin which is located at the center of the detonation. The TORT x- and y-axes are also aligned with the HPAC source geometry.

**Table 3.4. ANSI standard dose rate and protection factors for driver's head position as a function of vehicle location and orientation (no contributions from fallout on vehicle).**

Vehicle Location (m) <sup>a</sup>		Vehicle Orientation Angle (deg.)	Free-Field Dose Rate (mrem/h)	Shielded Dose Rate (mrem/h)	Protection Factor
x	y				
-100.0	-50.0	0	19.62	3.412	5.752
		90	19.20	3.084	6.225
		180	19.48	2.265	8.600
		270	19.92	2.969	6.710
0.0	-50.0	0	56.81	8.167	6.957
		90	53.83	9.001	5.981
		180	53.30	7.056	7.554
		270	56.15	5.683	9.880
10.0	10.0	0	3873.0	150.1	25.80
		90	4294.0	293.0	14.66
		180	3407.0	329.0	10.36
		270	3089.0	206.6	14.95
-200.0	100.0	0	12.05	1.911	6.304
		90	11.92	1.550	7.691
		180	12.18	1.389	8.767
		270	12.31	1.746	7.052
-400.0	200.0	0	1.309	0.2108	6.210
		90	1.300	0.1693	7.680
		180	1.322	0.1489	8.879
		270	1.331	0.1910	6.968
-400.0	400.0	0	2.807	0.3269	8.589
		90	2.771	0.2804	9.883
		180	2.828	0.2613	10.82
		270	2.865	0.3063	9.353
400.0	400.0	0	0.1980	0.02131	9.293
		90	0.2001	0.02940	6.807
		180	0.1976	0.03314	5.963
		270	0.1955	0.02855	6.848

<sup>a</sup>The vehicle locations are with respect to the TORT origin which is located at the center of the detonation. The TORT x- and y-axes are also aligned with the HPAC source geometry.

**Table 3.5. ANSI standard dose rate and protection factors for driver's head position as a function of vehicle location and orientation (includes contributions from fallout on vehicle).**

Vehicle Location (m) <sup>a</sup>		Vehicle Orientation Angle (deg.)	Free-Field Dose Rate (mrem/h)	Shielded Dose Rate (mrem/h)	Protection Factor
x	y				
-100.0	-50.0	0	19.62	3.420	5.739
		90	19.20	3.091	6.211
		180	19.48	2.273	8.571
		270	19.92	2.977	6.691
0.0	-50.0	0	56.81	8.403	6.761
		90	53.83	9.206	5.848
		180	53.30	7.262	7.339
		270	56.15	5.924	9.478
10.0	10.0	0	3873.0	490.2	7.902
		90	4294.0	642.3	6.686
		180	3407.0	580.4	5.870
		270	3089.0	435.5	7.093
-200.0	100.0	0	12.05	2.014	5.983
		90	11.92	1.649	7.232
		180	12.18	1.492	8.164
		270	12.31	1.853	6.645
-400.0	200.0	0	1.309	0.2186	5.988
		90	1.300	0.1769	7.349
		180	1.322	0.1568	8.436
		270	1.331	0.1990	6.688
-400.0	400.0	0	2.807	0.4730	5.935
		90	2.771	0.4246	6.527
		180	2.828	0.4091	6.913
		270	2.865	0.4561	6.282
400.0	400.0	0	0.1980	0.02132	9.288
		90	0.2001	0.02941	6.804
		180	0.1976	0.03315	5.961
		270	0.1955	0.02856	6.845

<sup>a</sup>The vehicle locations are with respect to the TORT origin which is located at the center of the detonation. The TORT x- and y-axes are also aligned with the HPAC source geometry.

**Table 3.6. ANSI standard dose rate and protection factors for driver's head position as a function of vehicle location and orientation (includes contributions from fallout on vehicle and on ground inside MASH-MORSE geometry model).**

Vehicle Location (m) <sup>a</sup>		Vehicle Orientation Angle (deg.)	Free-Field Dose Rate (mrem/h)	Shielded Dose Rate (mrem/h)	Protection Factor
x	y				
-100.0	-50.0	0	19.62	3.421	5.736
		90	19.20	3.092	6.208
		180	19.48	2.274	8.566
		270	19.92	2.978	6.688
0.0	-50.0	0	56.81	8.444	6.728
		90	53.83	9.245	5.823
		180	53.30	7.303	7.298
		270	56.15	5.969	9.406
10.0	10.0	0	3873.0	558.0	6.941
		90	4294.0	696.8	6.163
		180	3407.0	628.7	5.419
		270	3089.0	484.8	6.373
-200.0	100.0	0	12.05	2.033	5.927
		90	11.92	1.667	7.151
		180	12.18	1.512	8.059
		270	12.31	1.872	6.575
-400.0	200.0	0	1.309	0.2200	5.948
		90	1.300	0.1784	7.290
		180	1.322	0.1582	8.358
		270	1.331	0.2005	6.639
-400.0	400.0	0	2.807	0.5000	5.615
		90	2.771	0.4517	6.136
		180	2.828	0.4368	6.475
		270	2.865	0.4836	5.924
400.0	400.0	0	0.1980	0.02132	9.287
		90	0.2001	0.02941	6.804
		180	0.1976	0.03315	5.961
		270	0.1955	0.02856	6.845

<sup>a</sup>The vehicle locations are with respect to the TORT origin which is located at the center of the detonation. The TORT x- and y-axes are also aligned with the HPAC source geometry.

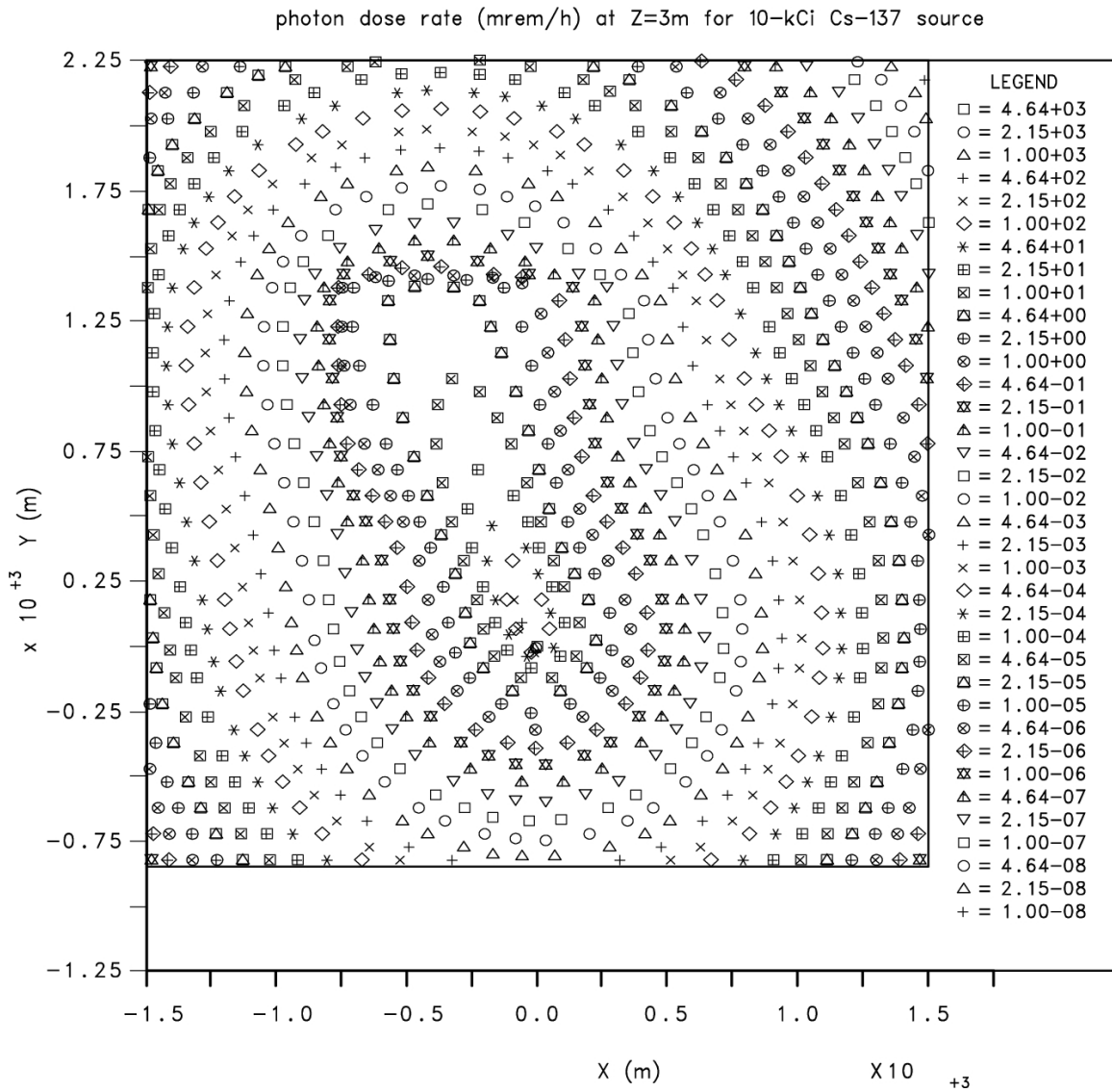


**Figure 3.1. Photon isodose-rate contours for a horizontal plane 3m above the ground due to the detonation and dispersal of a 10-kCi <sup>137</sup>Cs source.**

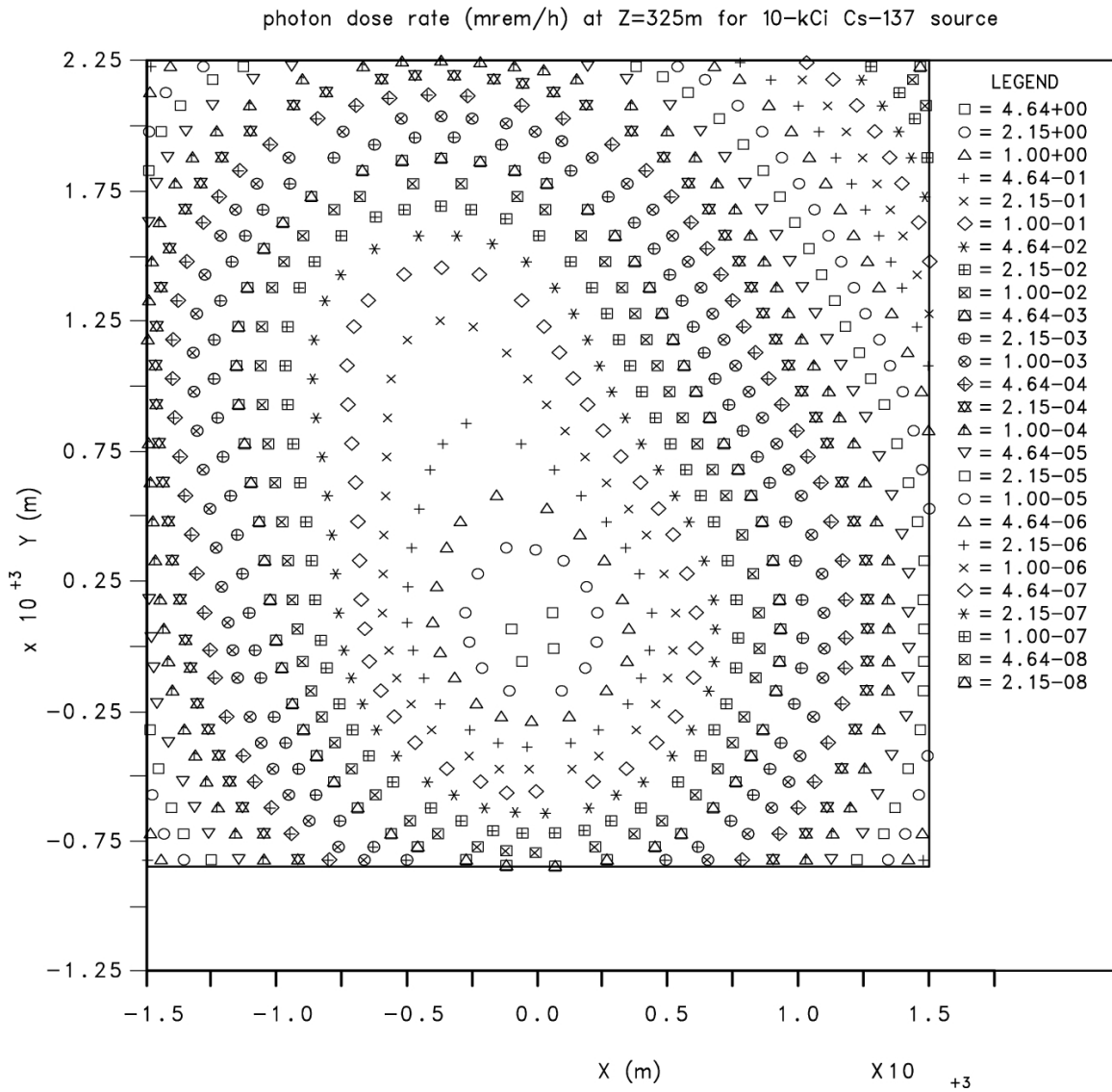


**Figure 3.2. Photon isodose-rate contours for a horizontal plane 325m above the ground due to the detonation and dispersal of a 10-kCi <sup>137</sup>Cs source.**

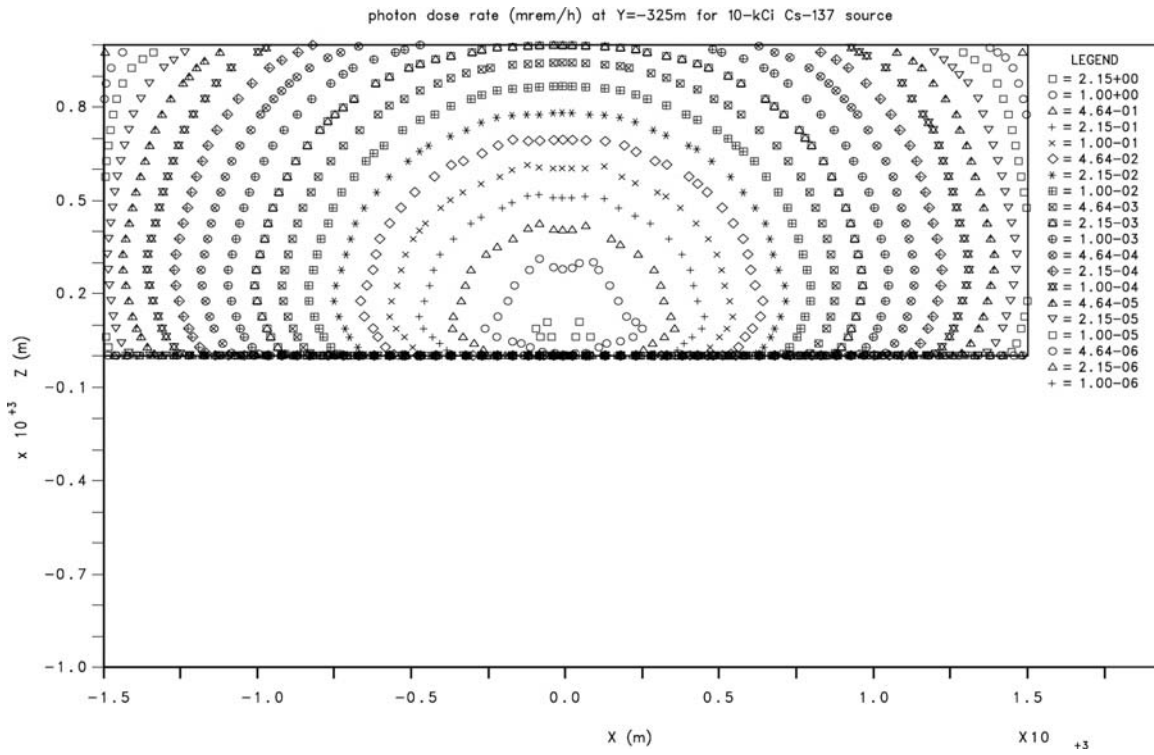


**Figure 3.3. Photon isodose-rate contours for a vertical plane 325m left of the origin due to the detonation and dispersal of a 10-kCi <sup>137</sup>Cs source.**

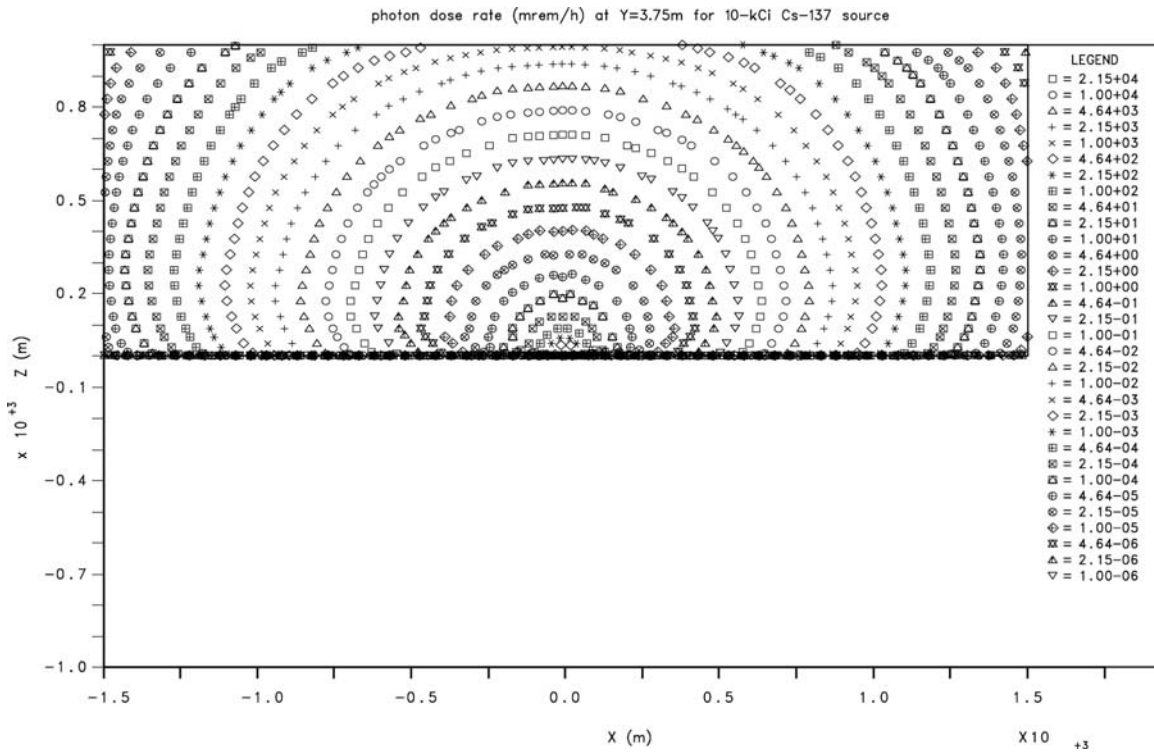


**Figure 3.4. Photon isodose-rate contours for a vertical plane 3.75m right of the origin due to the detonation and dispersal of a 10-kCi <sup>137</sup>Cs source.**

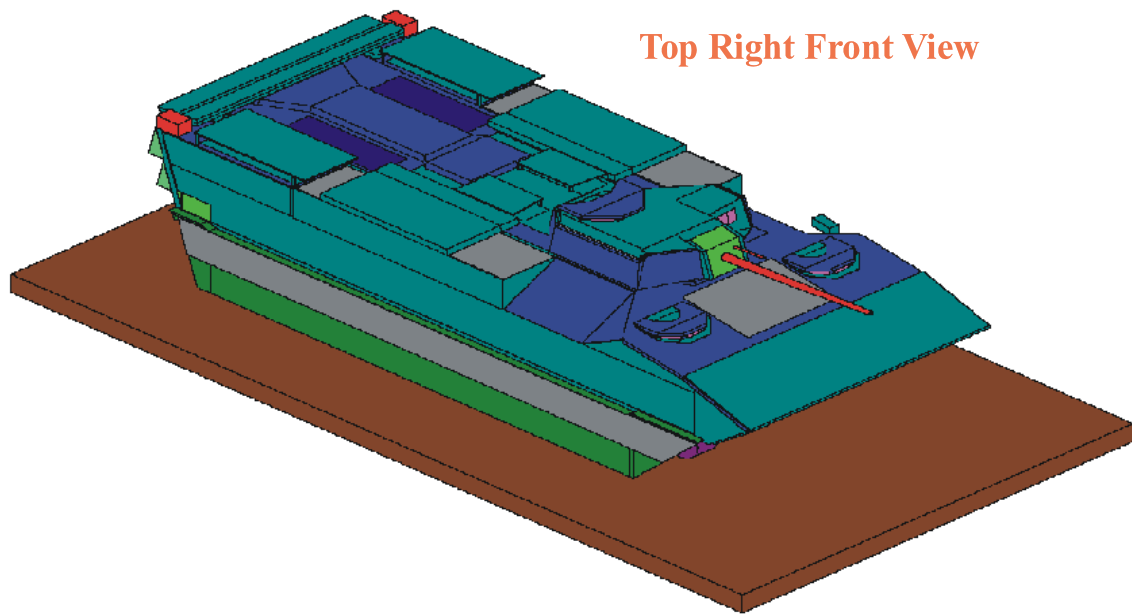


**Figure 3.5. Model of the composite material armored assault vehicle used in the analysis.**

## Cut-Away View Of Crew And Marine Positions

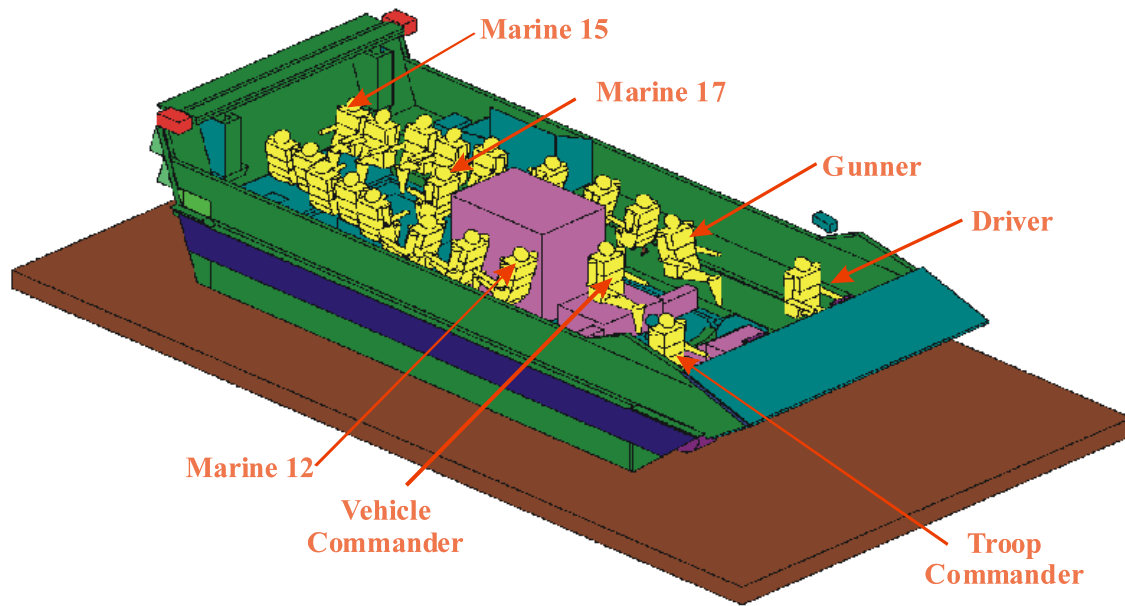


**Figure 3.6.** Cutaway view of the model of the composite material armored assault vehicle used in the analysis. The model shows the crew and infantry locations.

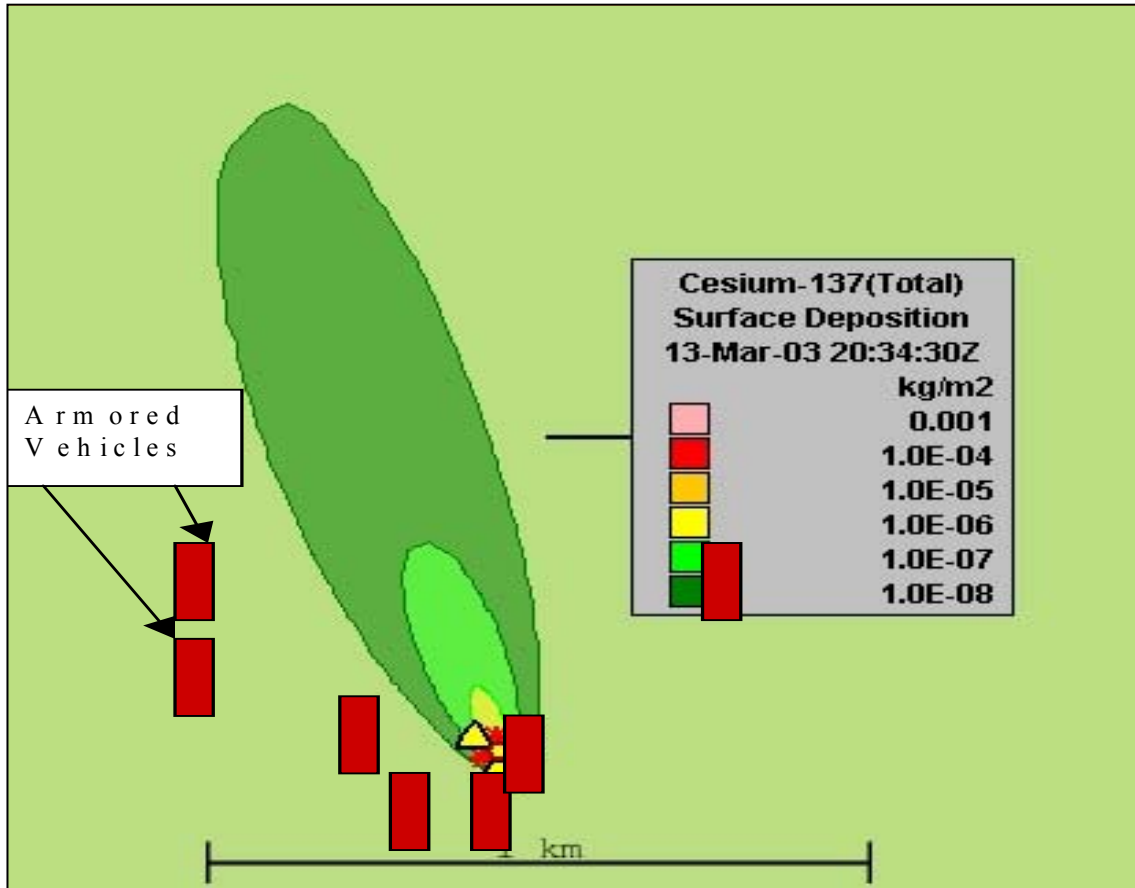


**Figure 3.7.** Approximate locations of the armored vehicle within the radiation field for the results shown in Tables 3.1-3.7.

Spectra for Cmdr's Head in Vehicle Near 10-kCi  $^{137}\text{Cs}$  Explosion

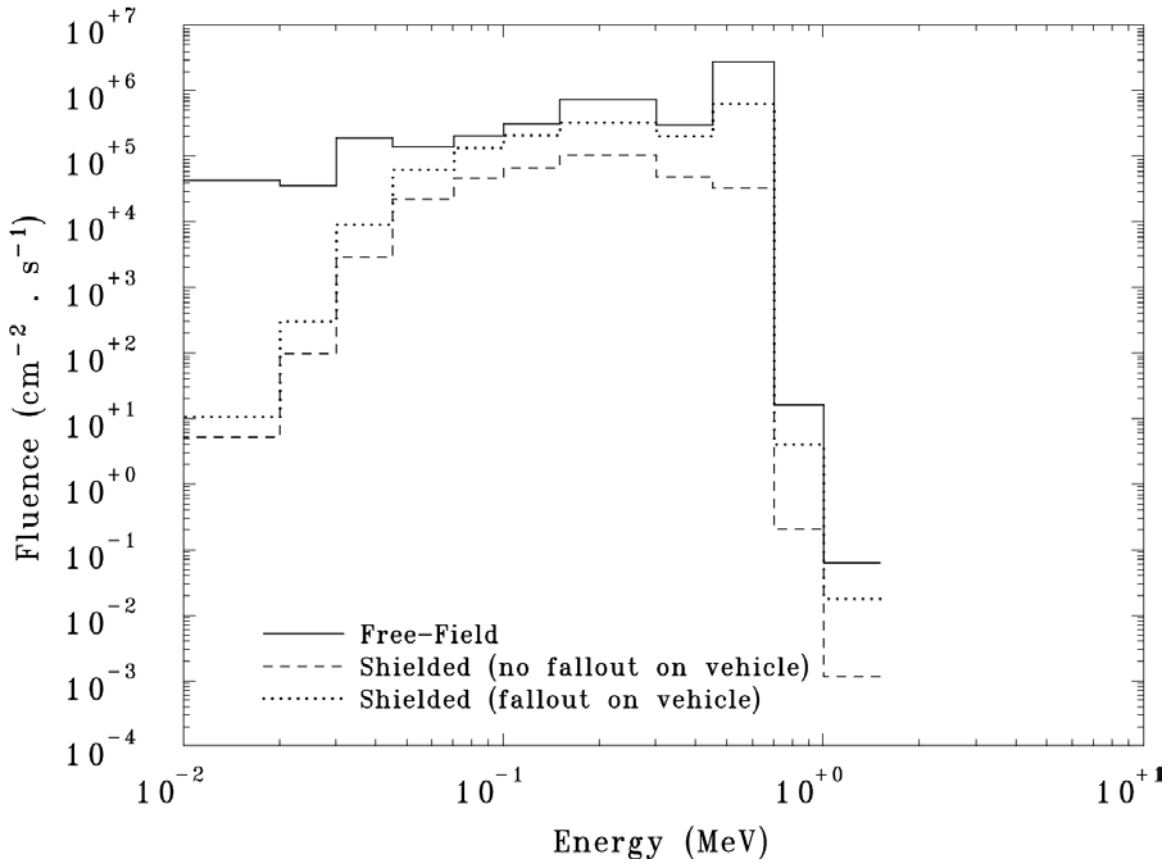


Figure 3.8. Free-field and shielded fluence spectra at the commander's head position for a vehicle located near the detonation site for the 10-kCi  $^{137}\text{Cs}$  weapon ( $x=10$  m and  $y=10$  m,  $0^\circ$  orientation angle).

Spectra for Cmdr's Head in Vehicle Far From 10-kCi  $^{137}\text{Cs}$  Explosion

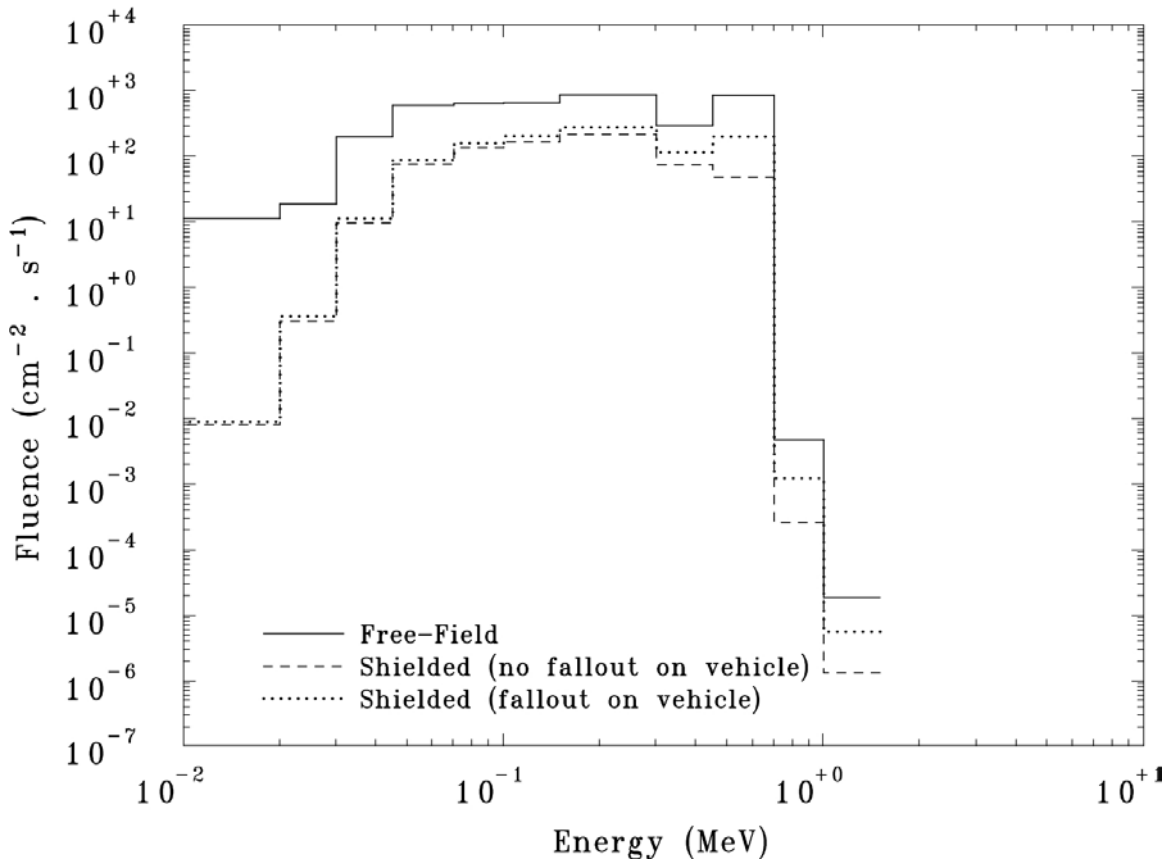


Figure 3.9. Free-field and shielded fluence spectra at the commander's head position for a vehicle located at a large distance from the detonation site for the 10-kCi  $^{137}\text{Cs}$  weapon ( $x=-400$  m and  $y=400$  m,  $0^\circ$  orientation angle).

Page Intentionally Blank

## 4.0 CONCLUSIONS

A brief study of the radiation effects from the detonation of a so-called dirty bomb was carried out. The event was modeled in the HPAC code system to create a dispersal pattern and generate a source distribution that could be used to prepare a source for the TORT radiation transport code. The TORT calculation was run to obtain free-field air-over-ground fluences. In addition, adjoint MASH-MORSE calculations were run for two detector locations within an armored vehicle. Adjoint leakages from the vehicle were coupled to the free-field fluences to calculate quantities of interest at those detector locations as well as protection factors offered by the vehicle as a function of location and orientation within the fluence field. In addition, contributions from fallout on the top surfaces of the vehicle were examined. The calculations demonstrated that using a computer like our fastest IBM workstation, one can obtain meaningful results within a reasonable amount of time. At the same time, because of the steep gradients in the source distribution, the approximate method in DRC4B is not very useful as a tool to check the DRC3B results, since it appears to severely underestimate the radiation levels. Protection factors can vary widely depending upon the location and orientation of the vehicle with respect to the detonation point. At one location near the detonation point when fallout on the vehicle was not considered, we saw a factor of 2.9 variation as a function of orientation for the commander's head position and a factor of 2.5 for the driver's head position. Variations for the other locations were much smaller.

Page Intentionally Blank

## 5.0 REFERENCES

1. NATO Army Armaments Group, "Guidelines for the Military Vehicle Designer to Improve Nuclear Radiation Protection," Allied Engineering Publication AEP-14, Edition 4 (May 2003).
2. Defense Threat Reduction Agency, *Hazard Prediction and Assessment Capability (HPAC) User Guide Version 4.0.1*, (2002).
3. J. O. Johnson, editor, "A User's Manual for MASH v2.0 – A Monte Carlo Adjoint Shielding Code," Oak Ridge National Laboratory, ORNL/TM-11778/R2 (1999).
4. A. G. Croff, "ORIGEN2 – A Revised and Updated Version of the Oak Ridge Isotope Generation and Depletion Code," ORNL-5621 (1980) and A. G. Croft, "User's Manual for the ORIGEN2 Computer Code," ORNL/TM-7175 (1980).
5. J. P. Renier (ORNL), The GENMASH code is an undocumented auxiliary code used with HPAC to produce an interface file for coupling with the MASH system (1998).
6. C. O. Slater, J. M. Barnes, J. O. Johnson, J. P. Renier, and R. T. Santoro, "Coupling of MASH-MORSE Adjoint Leakages with Space- and Time-Dependent Plume Radiation Sources," ORNL/TM-2000/335 (April 2001).
7. W. A. Rhoades and R. L. Childs, "The TORT Three-Dimensional Discrete Ordinates Neutron/Photon Transport Code," Oak Ridge National Laboratory, ORNL-6268 (November 1987).
8. D. T. Ingersoll, R. W. Roussin, C. Y. Fu, and J. E. White, "DABL69: A Broad-Group Neutron/Photon Cross-Section Library for Defense Nuclear Applications," ORNL/TM-10568 (June 1989).
9. M. B. Emmett, "The MORSE Monte Carlo Radiation Transport Code System," ORNL-4972/R1 (February 1983).

Page Intentionally Blank

**DISTRIBUTION LIST****Internal**

S. T. Baker	J. O. Johnson	J-P. A. Renier	J. D. White
J. M. Barnes	R. A. Lillie	A. W. Riedy	B. A. Worley
V. M. Baylor	R. E. McCauley	R. A. Sanders	Central Research Library
E. D. Blakeman	G. E. Michaels	R. T. Santoro (10)	Laboratory Records (RC)
J. C. Gehin (5)	R. H. Morris	L. J. Satkowiak	Office of Scientific and
W. H. Gray	B. D. Patton	C. O. Slater (5)	Technical Information
David J. Hill	D. E. Peplow	C. D. Sulfredge	(OSTI)
D. T. Ingersoll	I. Remec	J. M. Whitaker	

**External**

DAVIDSON, Dr. Charles N.  
 Director  
 U.S. Army Nuclear and Chemical Agency  
 7150 Heller Loop, Suite 101  
 Springfield, VA 22150-3198  
 UNITED STATES

DHERMAIN, Dr. Joël  
 Direction Des Centres D'Expertise et  
 D'Essais  
 Centre D'Etudes Du Bouchet  
 91710 Vert-Le-Petit  
 FRANCE

FLEMING, Dr. Mike A.  
 Technical Director  
 SERCO Assurance  
 Radiac Project Office, B150  
 Harwell, Oxon, OX11 0QJ  
 UNITED KINGDOM

HANN, Mr. Todd  
 Consequence Assessment Branch  
 Defense Threat Reduction Agency  
 Attn: TDOC  
 8725 John J. Kingman Road Stop 6201  
 Ft. Belvoir, VA 22060-6201  
 UNITED STATES

HASLIP, Dr. Dean  
 Defense Scientist  
 Defense R&D Canada – Ottawa  
 Ottawa, Ontario K1A 0Z4  
 CANADA

HEIMBACH, Dr. Craig R.  
 Chief, Army Pulse Radiation Facility  
 Army Pulse Radiation Facility  
 400 Collieran Road  
 Aberdeen Proving Ground, MD 21005-5059  
 UNITED STATES

KEHLET, Mr. Robert A.  
 Chief, Consequence Assessment Branch  
 Defense Threat Reduction Agency  
 Attn: TDOC  
 8725 John J. Kingman Road Stop 6201  
 Ft. Belvoir, VA 22060-6201  
 UNITED STATES

RAMBOUSKY, Major Ronald  
 Wehrwissenschaftliches Institut fuer  
 Schutztechnologien – ABC-Schutz (WIS)  
 Humboldtstrasse  
 29633 Munster  
 GERMANY

SCHAENZLER, Dr. Ludwig  
 Wehrwissenschaftliches Institut fuer  
 Schutztechnologien – ABC-Schutz (WIS)  
 Humboldtstrasse  
 29633 Munster  
 GERMANY

SMITH, Dr. Christopher J.  
 Section Manager  
 SERCO Assurance  
 Thomson House Risley  
 Warrington WA3 6AT  
 UNITED KINGDOM

Page Intentionally Blank